THE ASTROPHYSICAL JOURNAL, 204:717–730, 1976 March 15

HIGH-FREQUENCY STRUCTURE OF OOTY OCCULTATION SOURCES. I. SOURCES WITH CENTRAL COMPONENTS

T. K. MENON*
National Radio Astronomy Observatory,† Green Bank, West Virginia
Received 1975 July 30; revised 1975 September 5

ABSTRACT

The NRAO three-element interferometer operating simultaneously at 2695 and 8085 MHz has been used to study 39 Ooty occultation sources which have been found to be double at 327 MHz. This paper reports on the comparison of the high- and low-frequency structures of five out of nine of the above sources which show an additional central component at the high frequencies. The spectral indices (below 10 GHz) of the central components vary from being positive, nearly zero to negative values as high as -0.65. The indices of the extended components are all steeper than about -0.9. Two of the sources are also shown to have compact subcomponents within the extended components. The fraction of the total flux density within the central components of the present sample of 39 weak sources appears to be higher than among the brighter sample of 3C sources.

Subject headings: radio sources: general — radio sources: spectra

I. INTRODUCTION

The Ooty radio telescope has been used to observe the lunar occultations of about 400 radio sources down to a flux limit of about 0.2 jansky at 327 MHz. The results of the analysis of the data for about 200 sources either have been published or are in the process of publication (see Kapahi, Gopal-Krishna, and Joshi 1974 for the most recent list of references to earlier lists). The radio positions derived from occultations generally have an accuracy of about 1″ in both coordinates. The effective resolutions obtained vary from about 1″ to a few arc seconds depending on the signal-to-noise ratio for the source.

The Ooty occultation data have provided for the first time detailed structural information at low frequencies for a large number of sources. Comparison of the structures at low frequencies with similar data at high frequencies should provide information of great interest for a physical understanding of the source mechanisms and their evolution. Such high-resolution information at high frequencies is as yet limited mostly to a number of the stronger and northern sources not covered by the lunar path. Hence a program has been initiated to observe a representative sample of occultation sources using the three-element interferometer system (Hogg *et al.* 1969) of the National Radio Astronomy Observatory.

II. OBSERVATIONS

This paper reports on the results of the comparison of the low- and high-frequency data for five of the sources which are prominent doubles at low frequency but have triple structures at high frequency. The sources were observed in the interferometer configuration 900–1800–2700 meters or 800–1900–2700 meters at both 2695 MHz (S-band) and 8085 MHz (X-band). The hour angle coverage for the various sources is indicated in Table 1. The observed visibility functions from the three-element system were inverted into brightness distributions and subsequently cleaned using a computer program developed by Balick and Fomalont (1973). Because of the incomplete baseline coverage of the observations, the parameters of the source components were determined by a model fitting program developed by Balick and Fomalont (1973). The positions, sizes, and fluxes of the components determined from the maps were used as inputs for the model fitting program and the parameters of the model were adjusted to minimize the residuals in the least squares sense. The parameters of the sources obtained by the above procedure are given in Table 1.

III. STRUCTURE RESULTS AND DISCUSSION OF SPECTRA

We shall first discuss the structures of individual sources obtained from lunar occultation data and compare these structures with that obtained at S-band and X-band.

a) 0341+251 (4C 25.13)

The structural data from four occultations of this source at Ooty has been interpreted by Kapahi *et al.* (1973) as that of a double source, the components of which are slightly elongated along the line joining them. The S-band and X-band maps derived from the present observations are shown in Figures 1*a* and 1*b*.

* On leave of absence from the Tata Institute of Fundamental Research, Bombay, 400005, India.

† Operated by Associated Universities, Inc., under contract with the National Science Foundation.

TABLE 1

Comparison of Lunar Occultation Data and Interferometer Data

Source	Hour Angle Range	Component		R.A. (1950)	Decl. (1950)	Flux Density, 2695 MHz (Jy)	Flux Density, 8085 MHz (Jy)
0341+251......	-5^h30^m to $+5^h40^m$	A	L.O.	$03^h41^m46^s.36 \pm 0.05$	$25°11'08''.2 \pm 0.7$		
			I	46.36 ± 0.07	09.7 ± 0.5	0.08	0.03
		B	L.O.	46.95 ± 0.04	$10\ 53.1 \pm 0.7$		
			I	47.02 ± 0.07	52.7 ± 0.5	0.07	0.02
		C	I	46.65 ± 0.07	$11\ 00.7 \pm 0.5$	0.07	0.04
0416+270......	-5^h40^m to $+5^h15^m$	A	L.O.	$04\ 16\ 04.98 \pm 0.15$	$27\ 05\ 18.6 \pm 2$		
			I	05.14 ± 0.21	25.3 ± 1.5	0.18	0.06
		B	L.O.	08.90 ± 0.3	$04\ 22.0 \pm 5$		
			I	08.71 ± 0.21	14.9 ± 1.5	0.09	0.03
		C	I	06.49 ± 0.10	$04\ 55.3 \pm 1.0$	0.22	0.16
0648+263......	-5^h30^m to $+5^h00^m$	A	L.O.	$06\ 48\ 33.81 \pm 0.04$	$26\ 19\ 49.9 \pm 0.5$		
			I	33.73 ± 0.07	51.6 ± 0.5	0.17	0.06
		B	L.O.	35.01 ± 0.04	53.2 ± 0.5		
			I	35.00 ± 0.07	53.6 ± 0.5	0.11	0.03
		C	I	34.62 ± 0.07	52.6 ± 0.5	0.14	0.08
0814...........	-5^h10^m to $+5^h10^m$	A	L.O.	$08\ 14\ 38.05 \pm 0.15$	$22\ 46\ 49.0 \pm 2$		
			I	37.90 ± 0.07	50.4 ± 0.5	0.18	0.06
		B	L.O.	38.35 ± 0.07	27.7 ± 1		
			I	38.26 ± 0.07	26.4 ± 0.5	0.50	0.20
		C		38.12 ± 0.07	38.4 ± 0.5	0.04	0.06
0850+140......	-5^h20^m to $+4^h45^m$	A	L.O.	$08\ 50\ 22.42 \pm 0.04$	$14\ 04\ 17.7 \pm 0.5$		
			I	22.35 ± 0.07	16.9 ± 0.5	0.20	0.07
		B	L.O.	23.17 ± 0.04	18.7 ± 0.5		
			I	23.11 ± 0.07	18.9 ± 0.5	0.82	0.18
		C	I	22.70 ± 0.07	16.0 ± 0.5	0.11	0.08

The positions of the two occultation components are also indicated on the X-band map. The position angle of the synthesized beam is so close to the position angle of the two components that the components are not fully resolved at S-band. However, the source is fully resolved at X-band and shows, in addition to the two occultation components (A, B), a third component (C) situated approximately at the center of the line joining the two outer components. There is also an indication of an extension of A toward C. This central component has nearly 44 percent of the total flux density of the source at X-band.

The spectral index of the whole source over the range 327 to 8085 MHz is found to be about -0.88 (Fig. 2). There is some indication of a flattening of the spectrum toward frequencies lower than 327 MHz. A plausible separation of the components using the flux ratio at 327 MHz and the observed fluxes at X-band suggests that the spectral indices of the components A and B are about -1.04 and 1.11, respectively. The spectral index of the central component C is about -0.53. There is no clear indication of the existence of the component C in the occultation records at 327 MHz due to the low signal-to-noise ratio of the data. Even though the occultation data suggest that components A and B may be elongated in P.A. 152, our present data are consistent with a model containing three unresolved components corresponding to A, B, and C. Further high-resolution low-frequency observations combined with VLBI observations at high frequencies are needed to determine whether the spectrum of component C turns over at low frequencies as is usual for compact sources.

No optical identification has yet been possible for the source, partly because of the overlying obscuration due to the Pleides group of dark clouds. However, the small angular extent of the source and the unresolved nature of the outer components suggest that the optical object is likely to be a high-redshift object.

b) 0416+270 (4C 27.13)

According to Joshi *et al.* (1974) the occultation data of this source can be interpreted as that of a double source with a component separation of 72″ in position angle 137°. There is also a possible third component between A and B with ≤ 20 percent of the total flux, about 29″ southeast of A along the line joining A and B. The angular sizes of the components A and B are given as $\sim 15''$ and $\leq 15''$, respectively, in P.A. 18° and $\sim 18''$ and $\sim 40''$ in P.A. 319°. The flux ratio of A to B is given as 2.4.

The interferometer map at S-band for the source is shown in Figure 3. The occultation positions of the components are also marked on the map. The occultation and interferometer positions of the components A and B do not agree as well as in the case of other sources and the disagreement may be due to spectral index variation within the components. Considering the extended nature of the components, such spectral-index variations are not unexpected. It is clear from the figure that the dominant component at S-band is a central component which is only weakly seen at 327 MHz. Because of the limited baseline coverage of the observations, the components A and B are mostly resolved out at X-band with only a fraction of the

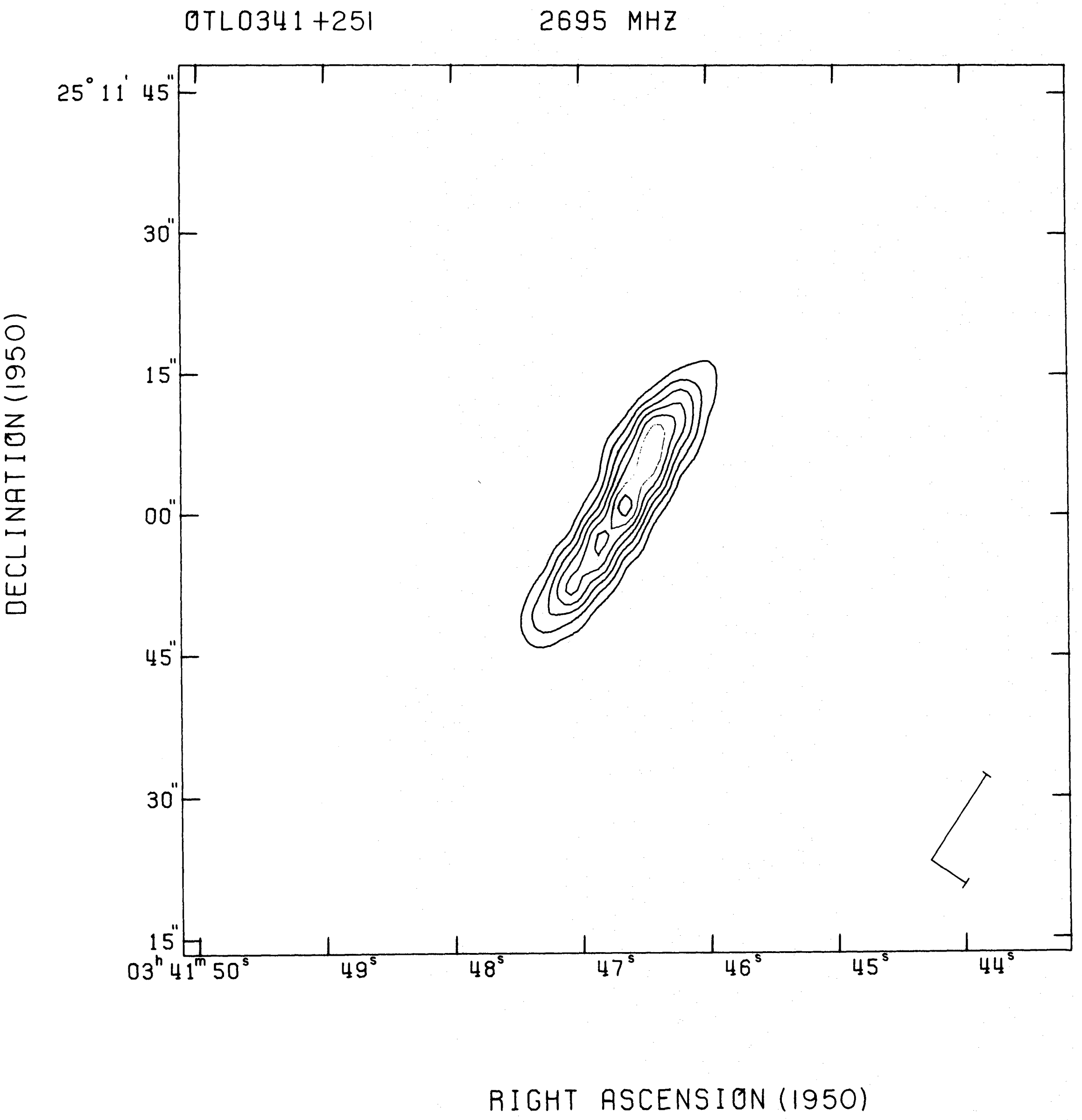

FIG. 1*a*.—Synthesized map of 0341+251 at 2695 MHz. The lowest contour and the contour intervals are 10 percent of peak brightness. The synthesized beam is 10″1 × 4″0 at a position angle of −38°0 and is shown to scale at the lower right-hand corner.

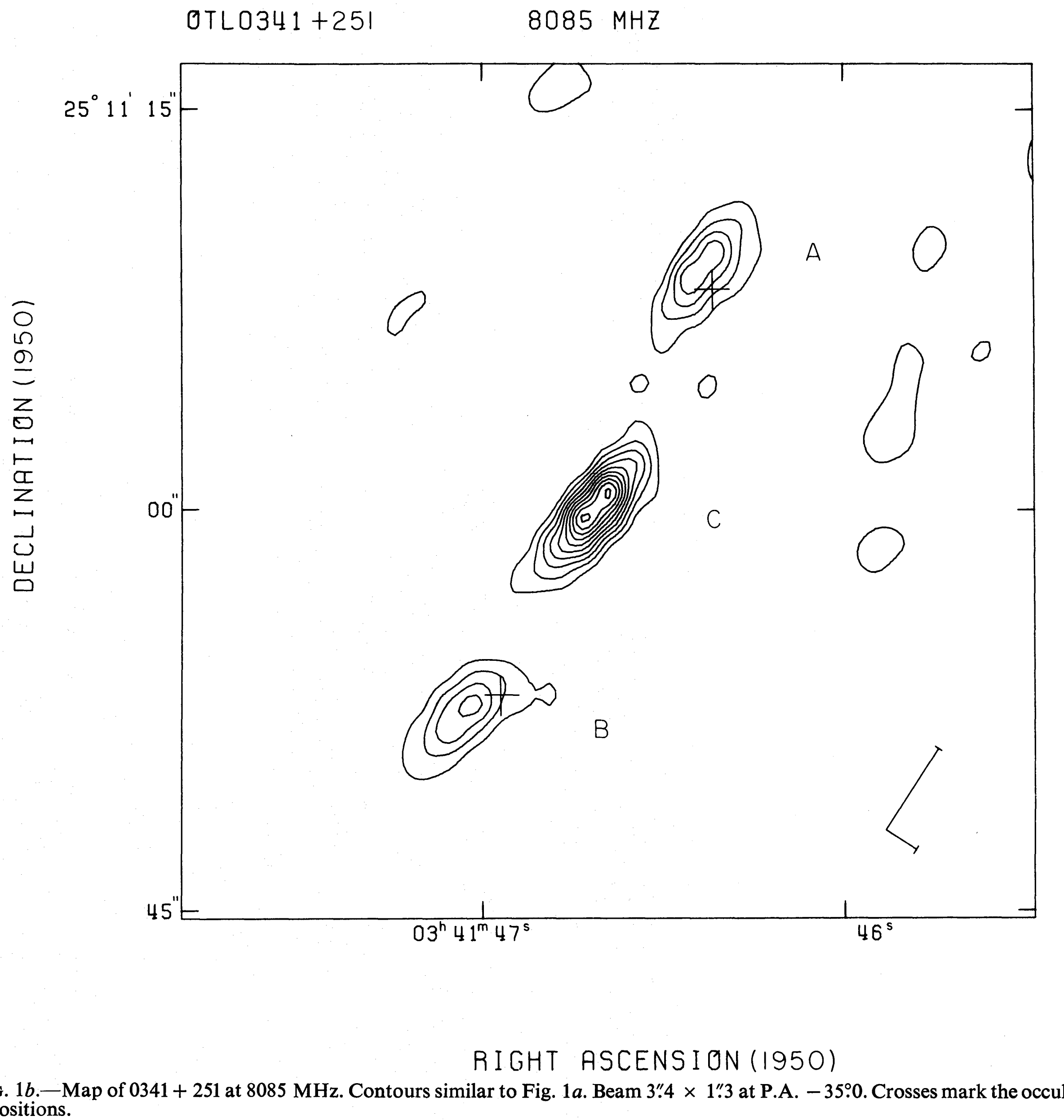

FIG. 1*b*.—Map of 0341 + 251 at 8085 MHz. Contours similar to Fig. 1*a*. Beam 3″.4 × 1″.3 at P.A. −35°.0. Crosses mark the occultation positions.

flux of component A being seen in the interferometer map.

Most of the total flux measurements from the source between 38 MHz and 2 GHz can be represented by a spectral index of about 0.88 (Fig. 4) with the measurement at 179 MHz being about 30 percent below the value expected for the above spectral index. Part of this discrepancy may be due to the reduced response of the synthesis instrument at 179 MHz to the wide double source of angular extent 85″ as compared with a single source assumed in the flux density measurement. It is also possible that the central component C becomes optically thick below about 300 MHz and hence its lower contribution below that frequency produces a kink in the spectrum. Perhaps both the effects contribute to the lower observed flux density at 179 MHz. The spectral index becomes flatter beyond about 2 GHz, which is again consistent with the increasing contribution of component C at higher frequencies. The spectral indices of components A, B, and C are −0.97, −0.9, and −0.37, respectively. Since a flat spectral index of −0.37 is rare (Kellermann, Pauliny-Toth, and Williams 1969), in reality component C most probably consists of a steep spectral-index halo and a self-absorbed core.

No optical identification of the source has yet been possible because of the high absorption in the field. The large angular extent of the source is suggestive of a comparatively nearby source. However, the dominance of the central component at high frequencies is quite unusual for such an extended source. A full synthesis of this source is necessary to determine the relationship of the outer components to the central component.

c) *0648+263* (*4C 26.25*)

The occultation data for this source as given by Kapahi *et al.* (1973) indicates a simple double source

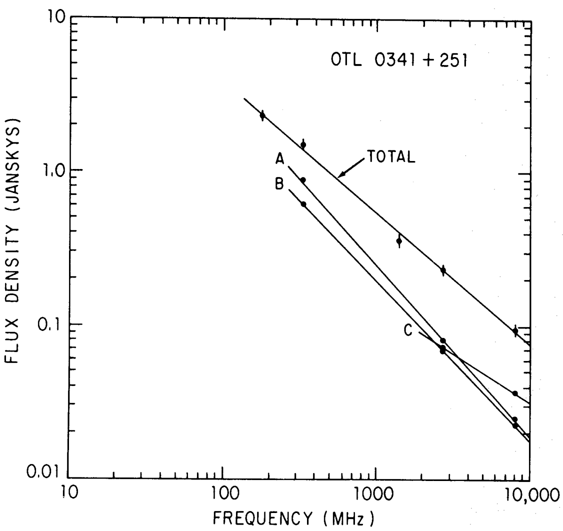

FIG. 2.—Spectrum of 0341+251. Sources of flux density data 179 MHz: Pilkington and Scott 1965. 327 MHz: Corrected Ooty data. (1400, 2695, 8085 MHz: Author's unpublished Green Bank data.)

with a flux density ratio of 0.9 and a separation of 16″.5 in P.A. 78°. The X-band map, Figure 5, shows that the source consists of three components, two of which (A, B) coincide with the occultation components and a third one (C) which is the strongest one at X-band. The flux density ratios A/B and C/Total are 2 and 0.47, respectively, at X-band. The total spectrum of the source, Figure 6, shows a definite kink in the spectrum beyond about 1400 MHz, suggesting that the spectrum of component C turns over below about 3 GHz. A plausible separation of the spectrum of the different components is shown in Figure 6. The spectral indices of A and B are approximately −0.86 and −1.13, respectively. The spectral index of C above 3 GHz is about −0.65. All the components appear unresolved even at X-band.

Kapahi *et al.* (1973) have suggested a 19.5 mag red galaxy as the likely optical identification. Their position for the galaxy, which is marked by a cross in Figure 5, and the position of component C agree to within 1″.5. No optical spectrum of the object is as yet available. From an analysis of the data on some 100 sources that were appreciably resolved at 1407 MHz by the Cambridge One-Mile telescope, Mackay (1971) had concluded that, in the case of double sources, the component that is fainter at 1407 MHz is almost always farther from the central object, has a steeper spectrum, and is less compact than the brighter component. However, in the case of 0648+263 we find that the brighter component A is about 12″ from the central component while the weaker component B is only 5″ from the center, even though (as noted earlier) the spectral index of A is flatter than that of B. The nearly collinear arrangement of the three components would appear to preclude the possibility that component A is unrelated to the other two components.

If the suggested identification with the 19.5 mag galaxy is correct, then, on the assumption that the absolute magnitude of a radio galaxy is −23.0 and a value of 55 km s^{-1} Mpc^{-1} for the Hubble constant, the distance of the source is about 300 Mpc and the linear separation AB about 40 kpc. The latter dimension is comparable to the diameter of a typical galaxy, and the occurrence of double sources of such small linear extent associated with galaxies is very rare. Since the absolute luminosity of the source at 179 MHz is only about 10^{26} W Hz^{-1} at the distance inferred above, most such sources will be at the detection limit of present low-frequency surveys, and structural information is available for very few such sources. In order to establish the reality of such a class of doubles, it is important to pursue the optical identification work for such sources.

The relationship of the turnover frequency, the maximum flux of a self-absorbed component and the magnetic field has been discussed by several authors (see Kellermann and Pauliny-Toth 1968). In the case of the present component C, the relationship is found to be

$$\theta^2 = 1.74 \times 10^{-6} H^{1/2} \tag{1}$$

where θ is in arc seconds and H is the magnetic field in

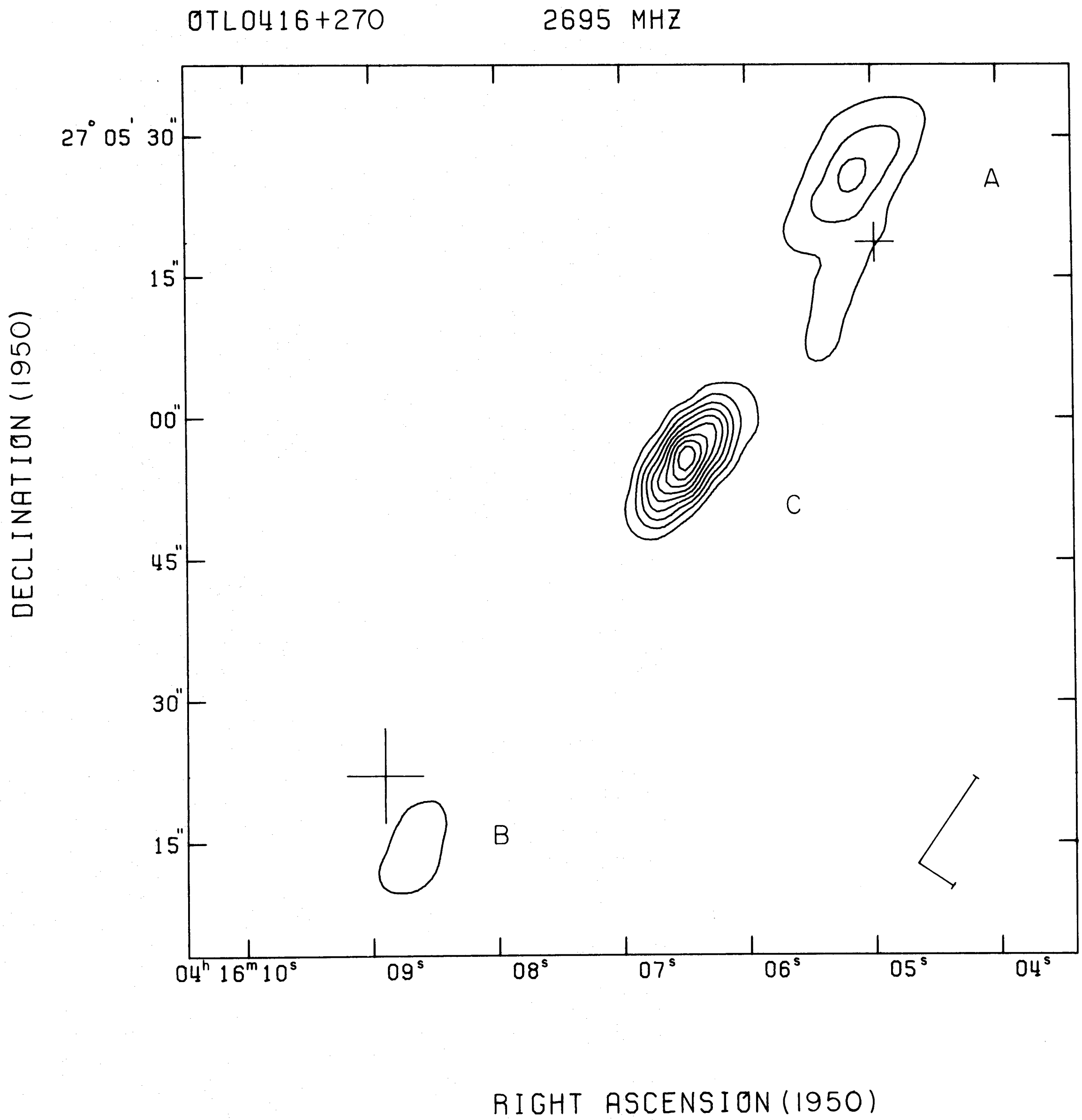

FIG. 3.—Map of 0416+270 at 2695 MHz. Contours similar to Fig. 1*a*. Beam 10″.8 × 4″.3 at P.A. −34°.0. Crosses mark the occultation positions.

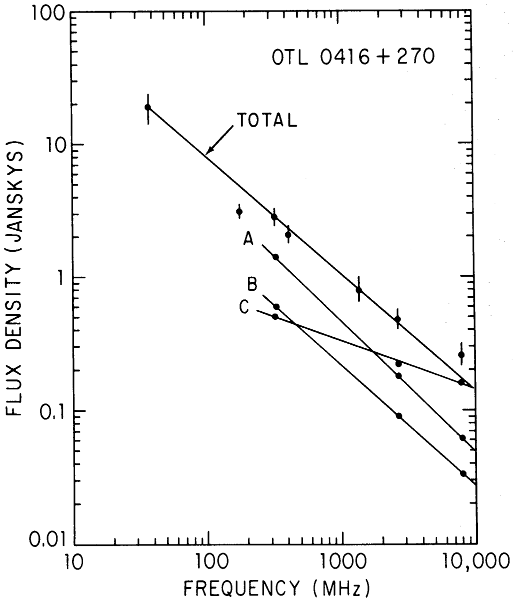

FIG. 4.—Spectrum of 0416+270. Sources of flux density data same as in Fig. 2.

gauss. A definitive measurement of the angular size of the component C using very large baseline interferometry can give useful information about the evolutionary stage of the component (Kellermann 1974).

d) *0814+227* (*4C 22.20*)

The occultation model of the source (see Kapahi *et al.* 1973) consists of two components, one of which (B) is stronger and more compact than the other one (A). The compact component B could have either a weak halo around it or two weak unresolved components within a few seconds of arc. The interferometer maps at S- and X-band are shown in Figures 7*a* and 7*b*, where the positions of the occultation components A and B are also marked. In addition to these two components, there is also a third component C which is particularly well seen at X-band. Components A and C are unresolved at X-band, but there is some suggestion that component B consists of an unresolved core and a weak halo as indicated also by the occultation data. The four-component model of the source derived by Wardle and Miley (1974) is not confirmed by the present observations.

The spectrum of the whole source given in Figure 8 is convex between 179 MHz and 8 GHz but turns up at lower frequencies. It is likely that the departure from a straight-line spectrum is due to systematic errors in the flux density data at low frequencies. A possible decomposition of the spectrum above 327 MHz into the three constituent components A, B and C (Fig. 8) can be made by using the observed fluxes at S- and X-band, the observed flux ratio at 327 MHz, and the fact that, according to Harris and Hardebeck (1969), 60 percent of the total flux at 408 MHz is in a scintillating component of less than 0″.2 diameter. It would appear from Figure 8 that this scintillating component is most likely to be part of component B. Since no structural information is available for frequencies below 327 MHz, it is difficult to infer the shapes of the component spectra below that frequency. If the change of slope in the total spectrum at about 200 MHz is real, it suggests that component B can be represented by a weak extended subcomponent with straight-line spectrum and a small-diameter subcomponent which radiates most of the flux at high frequencies and is optically thick at about 400 MHz. The high-frequency spectral indices of components A and B between 1 and 8 GHz are about -0.94 and -0.85, respectively. The flux density of component C is increasing toward high frequencies, and the maximum appears to occur beyond 8 GHz.

The position of component C coincides with that of the QSO suggested as the optical identification by Merkelijn, Shimmins, and Bolton (1968). The redshift z of this QSO has been measured by Schmidt (1974) as 0.980.

If we accept the turnover frequency of the subcomponent of B at 400 MHz as real, we can derive for this component the relationship given in equation (2) in a manner similar to equation (1):

$$\theta^2 = 3.94 \times 10^{-3} H^{1/2} . \tag{2}$$

It is clear from the above relation that, for almost any reasonable value of the magnetic field, the angular size of the subcomponent is much less than 1″. The existence of compact subcomponents within the extended outer components of Cygnus A has been noted by Miley and Wade (1971). In the present case the source has also a bright central component. A VLBI measurement of the angular size of the subcomponent of B should provide useful estimates of the time scale and confinement characteristics of the particles supplying the energy of the extended components themselves.

e) *0850+140* (*3C 208*)

The occultation data of this source have been interpreted by Joshi (1975) as that of a double source of total extent 11″ in position angle 85°. The sizes of the components A and B are respectively 6″ × 1.4″ and 1″.4 × 0″.8, and the flux density ratio A/B = 0.33.

The source has also been observed by Wilkinson, Richards, and Bowden (1974) using the 24 km baseline interferometer at Jodrell Bank, at 408 MHz and 610 MHz. Their model at 408 MHz consists of two components each of size 2″.3 × 1″.8 with a separation of 12″.4 and a flux density ratio of 0.15. These two components contain 88 percent of the total flux density at 408 MHz. The model at 610 MHz consists of two similar components each of size 1″.4 × 1″.4 with a separation of 11″.2 and a flux density ratio of 0.15, the two components accounting for 79 percent of the total flux. The differences between the occultation data and the above interferometer data may be attributed to the fact that the parameters from the interferometer

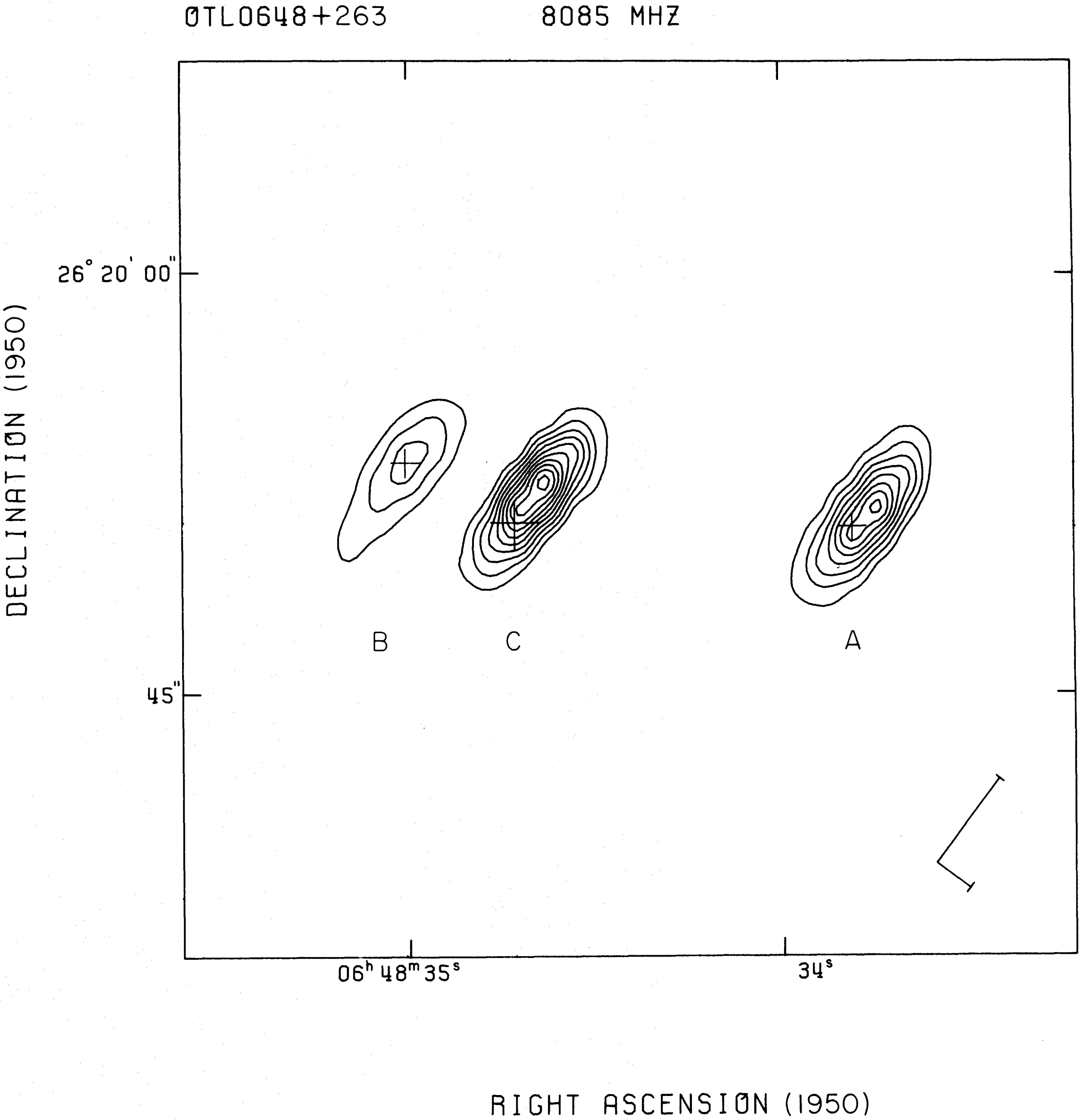

FIG. 5.—Map of 0648+263 at 8085 MHz. Contours similar to Fig. 1*a*. Beam 3".7 × 1".5 at P.A. −37°.0. Crosses near components A and B mark the occultation positions. The cross near C marks the position of the suggested optical identification.

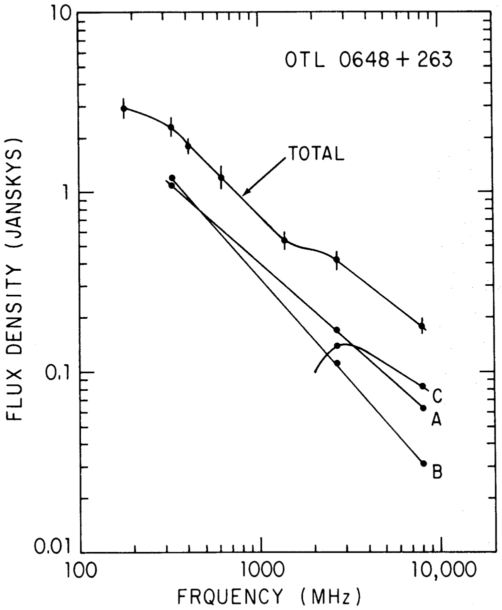

FIG. 6.—Spectrum of 0648+263. Sources of flux density data same as in Fig. 2.

data were obtained by a model fitting program using only two components. Also the observations were made for only one baseline.

The S- and X-band maps of the source are given in Figures 9*a* and 9*b*. The positions of the occultation components A and B agree very well with the positions of the two outer components at X-band. A third component C is also evident approximately at the center of the line forming A and B. The position of the QSO, suggested as the optical identification of the source by Sandage and Wyndham (1965), has been remeasured by Joshi (1975) and coincides with component C within observational errors. The redshift z of the QSO has been measured by Schmidt (1966) as 1.112.

The spectral index of the whole source is about -1.11 (Fig. 10) while the indices of the components A, B, and C are respectively -1.19, -1.16, and -0.25. However, there is some indication of flattening of the spectrum of the whole source at lower frequencies as indicated by the dashed line in Figure 10. The flux density ratio of components A and B is about 0.35 both at S- and X-band. Component C has about 24 percent of the total flux density at X-band, and all components are unresolved at X-band.

Interplanetary scintillation of the source at 81.5 MHz observed by Readhead and Hewish (1974) shows that 35 percent of the flux density of the source at 81.5 MHz is in a Gaussian component of diameter 0".7. Since the occultation data show that about 75 percent of the total density at 327 MHz is in component B, it seems likely that the scintillating part is within component B. At the distance corresponding to a redshift of 1.112 in an Einstein–de Sitter universe with $H_0 = 55$ km s^{-1} Mpc^{-1} the size of the scintillating component turns out to be about 1.6 kpc. This is comparable to the linear size of the hot spots found by Miley and Wade (1971) within the outer components of Cygnus A. In the present case, however, a much higher fraction of the total flux of the outer component B is in a compact structure even though the total luminosities of the two sources are comparable.

IV. DISCUSSION

In recent years high-resolution studies of a large number of extragalactic sources have shown that, even though a wide variety of structures exist among the bright sources, certain types of large-scale structures do predominate. For example, Mackay (1971) has concluded from an analysis of a complete sample of 199 3CR sources at 1407 MHz that at least 65 percent of sources have a double structure with two principal components. If we include the still higher resolution observations using the NRAO three-element interferometer and the 5 km Cambridge system, the fraction of sources which are double increases significantly. It should be emphasized here that the resolutions considered above are still only a few seconds of arc. The much higher resolutions obtained with the VLBI technique have shown that complex structures occur also inside sources whose total angular extent is less than 1". However, we are here concerned only with those extended sources with angular extents of a few seconds of arc.

Among the total of 79 sources selected from the Ooty occultation lists which were observed with the three-element interferometer, 39 were doubles of total angular extent greater than 4" at 327 MHz. Of these double sources, nine have been found to have central components which contain 20 percent or more of the total flux density at 8 GHz. These include the five sources discussed in the present paper as well as 3C 154 discussed by Menon (1975*a*) and two other sources (Menon 1975*b*). Since the vast majority of the 39 double sources in the present survey have flux densities below 0.5 Jy at 8 GHz, it is likely that a greater number of these sources have central components below the sensitivity limit of the present measurements. About 10 percent of all double sources are already known to have an additional bright component at the center which is also coincident with the optical object when an optical identification has been determined. It is, however, worth noting that among the more than 200 extended doubles observed with the 1 Mile telescope and the 5 km telescope at Cambridge (see MacDonald, Kenderdine, and Neville 1968; Branson *et al.* 1972; Harris 1972; Mackay 1969, 1971; Pooley and Henbest 1974) there are only about 10 sources whose central components contain more than 10 percent of the total flux density of the sources at 5 GHz. Of these only three sources, 3C 109, 3C 111 and 3C 207, are known to have central components containing more than 20 percent of the total flux density at 5 GHz. The data presented in this paper suggest that the weaker sources of the type investigated here may have greater activity in the center than the stronger sources. We have also seen that the spectral indices of the central

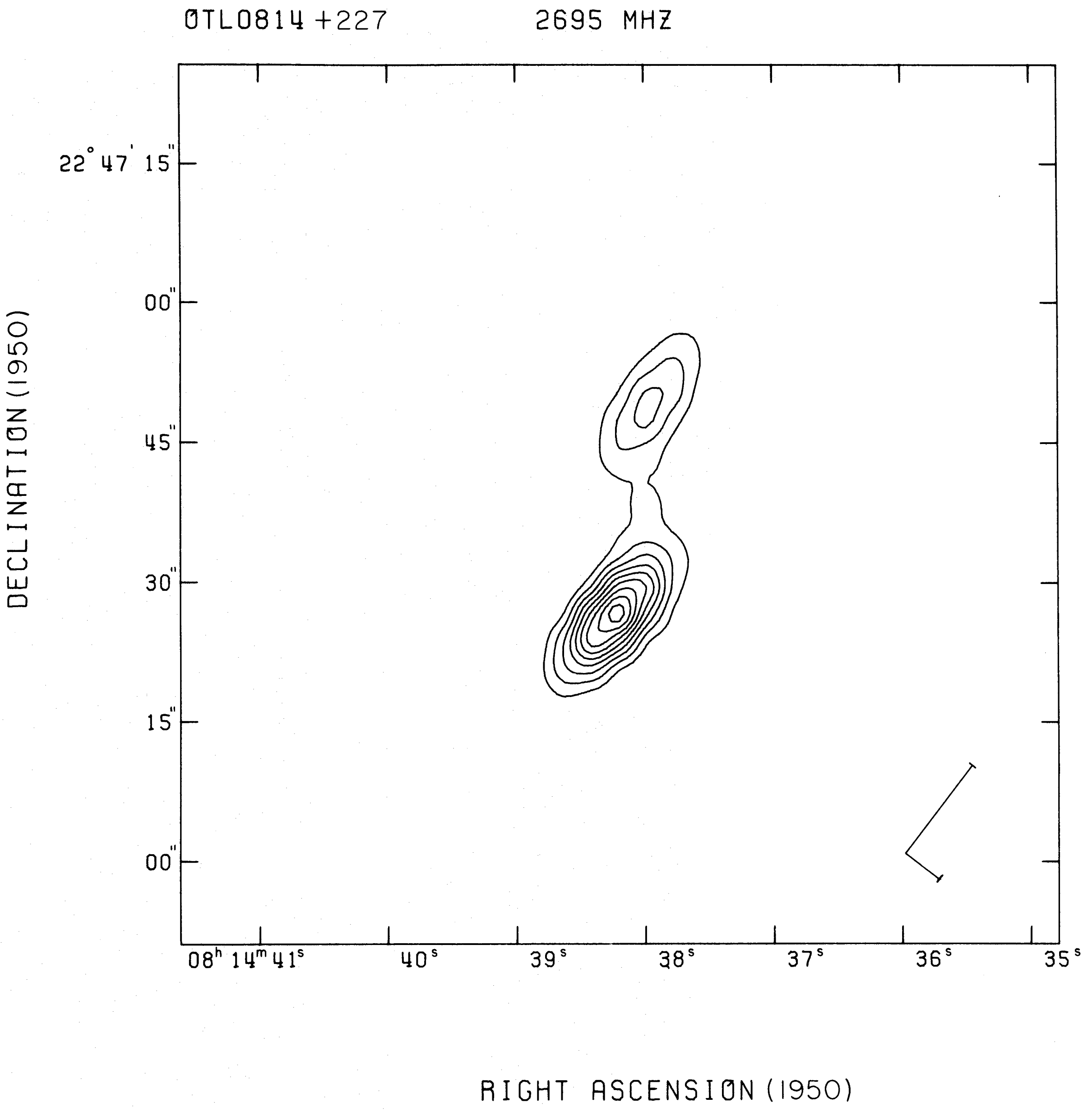

FIG. 7a.—Map of 0814+227 at 2695 MHz. Contours similar to Fig. 1a. Beam 11″.8 × 4″.8 at P.A. −38°.0.

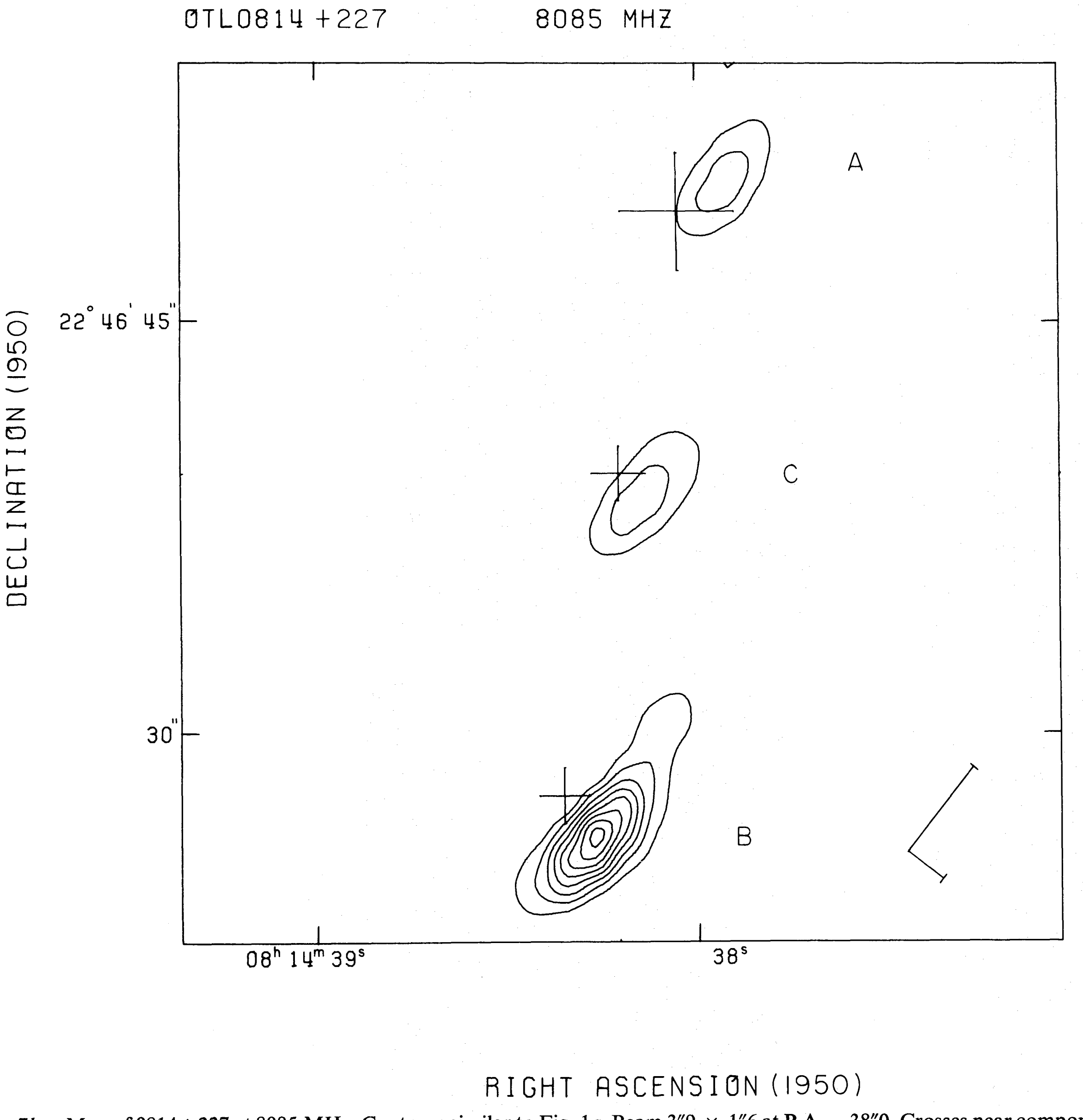

FIG. 7*b*.—Map of 0814+227 at 8085 MHz. Contours similar to Fig. 1*a*. Beam 3".9 × 1".6 at P.A. −38".0. Crosses near components A and B mark the occultation positions. The cross near C marks the position of the QSO.

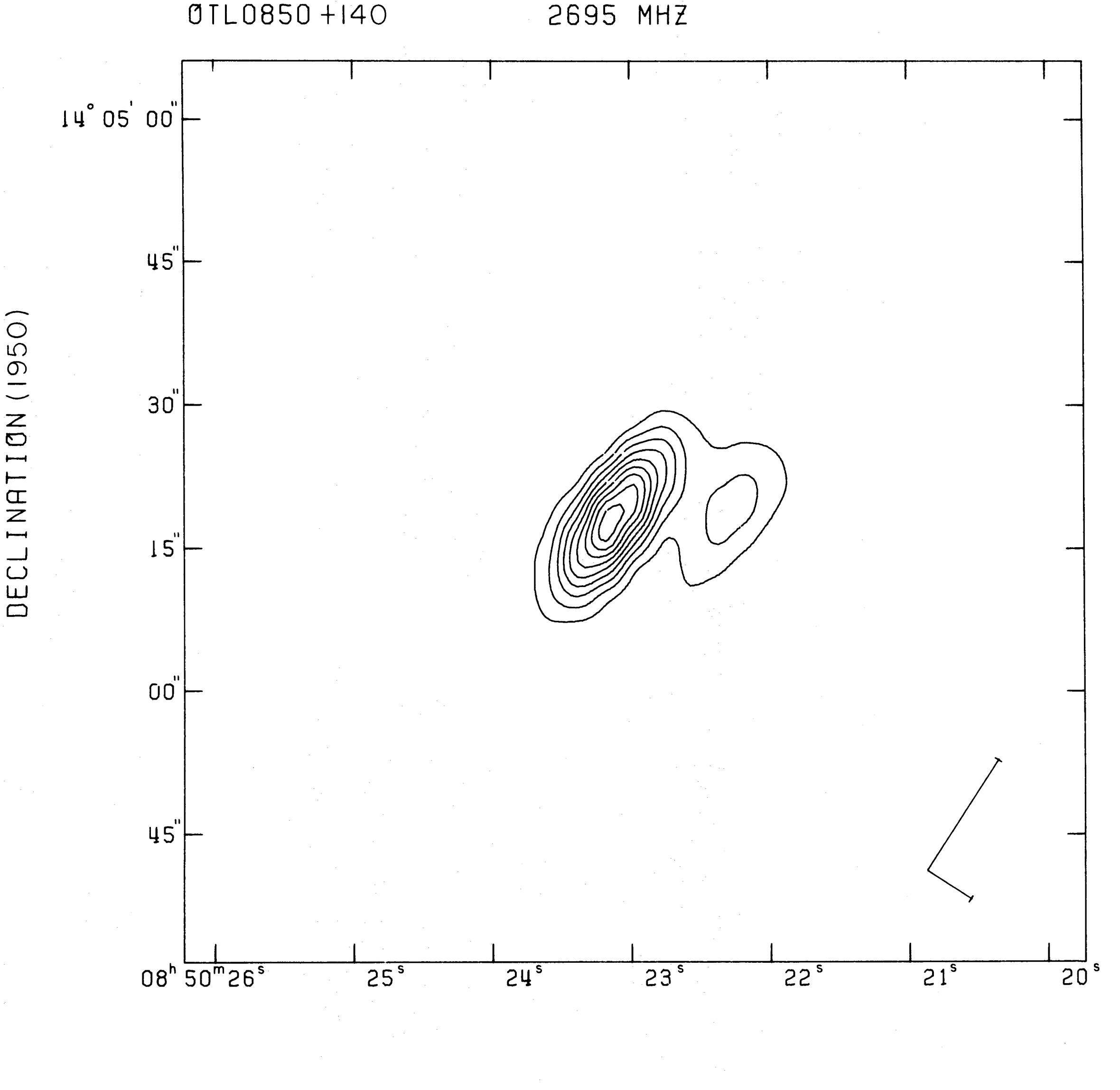

FIG. 9*a*.—Map of 0850+140 at 2695 MHz. Contours similar to Fig. 1*a*. Beam 13″.8 × 5″.5 at P.A. −33°.0.

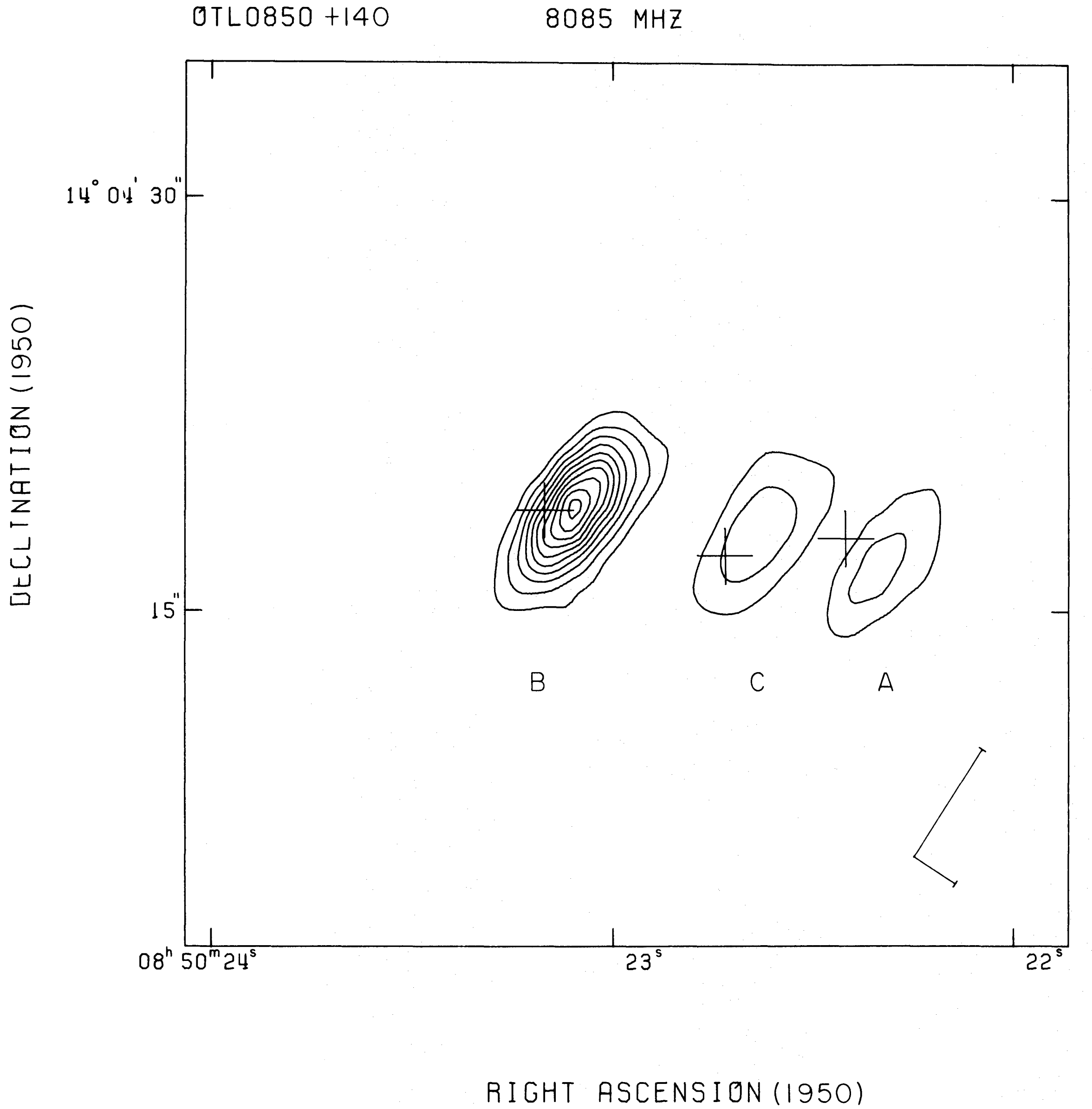

FIG. 9*b*.—Map of 0850+140 at 8085 MHz. Contours similar to Fig. 1*a*. Beam 4″6 × 1″8 at P.A. −33°0. Crosses near components A and B mark the occultation positions. The cross near C marks the position of the QSO.

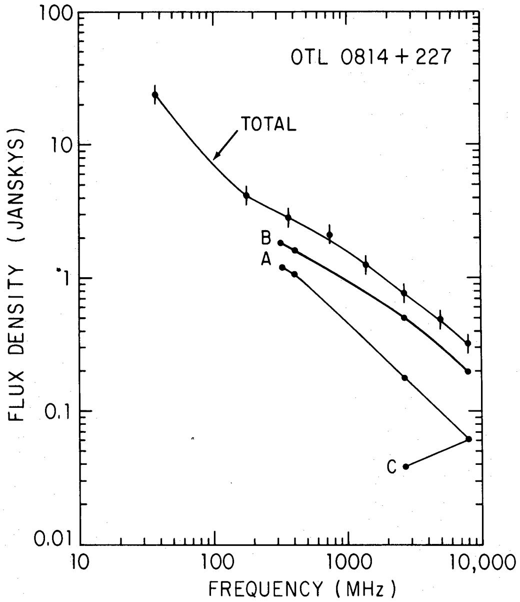

FIG. 8.—Spectrum of 0814+227. Sources of flux density data same as in Fig. 6 and at 5 GHz from Pauliny-Toth and Kellermann (1972).

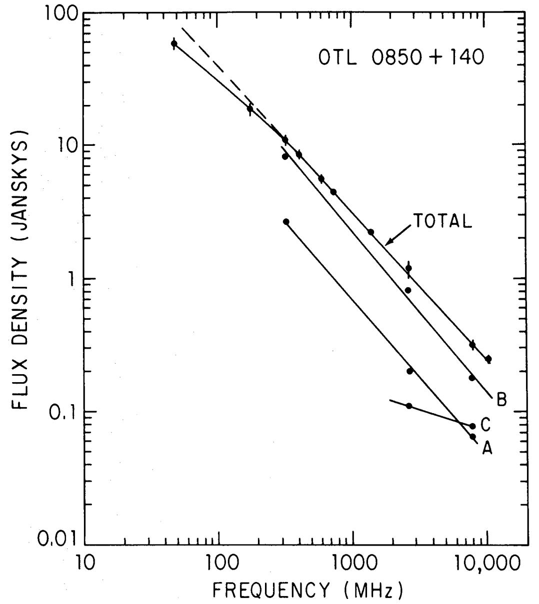

FIG. 10.—Spectrum of 0850+140. Sources of flux density data same as in Fig. 6 as well as Kellermann, Pauliny-Toth, and Williams (1969).

components below 10 GHz can be positive, nearly zero, or negative with an index as negative as −0.65. After subtracting the contribution of the central components, the spectral indices of the outer components are found to be generally steeper than about −0.9. The relationship of the central components to the extended components and their role in the evolution of double sources will be discussed elsewhere.

I am grateful to Dr. D. S. Heeschen, Director of NRAO, for a visiting appointment at NRAO which made this investigation possible. I wish to thank M. N. Joshi for communicating his analysis of the 3C 208 occultation data before publication.

REFERENCES

Balick, B., and Fomalont, E. B. 1973, NRAO Computer Division Internal Report No. 13.
Branson, N. J. B. A., Elsmore, B., Pooley, G. G., and Ryle, M. 1972, *M.N.R.A.S.*, **156**, 377.
Harris, A. 1972, *M.N.R.A.S.*, **158**, 1.
Harris, E. E., and Hardebeck, E. J. 1969, *Ap. J. Suppl.*, **10**, 115.
Hogg, D. E., Macdonald, G. H., Conway, R. G., and Wade, C. M. 1969, *A.J.*, **74**, 1206.
Joshi, M. N. 1975, personal communication.
Joshi, M. N., Kapahi, V. K., Gopal-Krishna, Sarma, N. V. G., and Swarup, G. 1974, *A.J.*, **79**, 515.
Kapahi, V. K., Joshi, M. N., Subramanya, C. R., and Gopal-Krishna. 1973, *A.J.*, **78**, 673.
Kapahi, V. K., Gopal-Krishna, and Joshi, M. N. 1974, *M.N.R.A.S.*, **167**, 299.
Kellermann, K. I. 1974, Galactic and Extragalactic Radio Astronomy (New York: Springer-Verlag), p. 320.
Kellermann, K. I., and Pauliny-Toth, I. I. K. 1968, *Ann. Rev. Astr. and Ap.*, **6**, 417.
Kellermann, K. I., Pauliny-Toth, I. I. K., and Williams, P. J. S. 1969, *Ap. J.*, **157**, 1.
Macdonald, G. H., Kenderdine, S., and Neville, A. C. 1968, *M.N.R.A.S.*, **138**, 259.
Mackay, C. D. 1969, *M.N.R.A.S.*, **145**, 31.
———. 1971, *ibid.*, **154**, 209.
Menon, T. K. 1975*a*, *Ap. J.*, in press.
———. 1975*b*, in preparation.
Merkelijn, J. K., Shimmins, A. J., and Bolton, J. G. 1968, *Australian J. Phys.*, **21**, 523.
Miley, G. K., and Wade, C. M. 1971, *Ap. Letters*, **8**, 11.
Pauliny-Toth, I. I. K., and Kellermann, K. I. 1972. *A.J.*, **77**, 797.
Pilkington, J. D. H., and Scott, P. F. 1965, *M.N.R.A.S.*, **69**, 183.
Pooley, G. G., and Henbest, S. N. 1974. *M.N.R.A.S.*, **169**, 47.
Readhead, A. C. S., and Hewish, A. 1974, *Mem. R.A.S.*, **78**, 1.
Sandage, A., and Wyndham, J. D. 1965, *Ap. J.*, **141**, 328.
Schmidt, M. 1966, *Ap. J.*, **144**, 443.
———. 1974, *ibid.*, **195**, 253.
Wardle, J. F. C., and Miley, G. K. 1974, *Astr. and Ap.*, **30**, 305.
Wilkinson, P. N., Richards, P. J., and Bowden, T. N. 1974, *Jodrell Bank Ann.*, Ser. 1, **2**, 250.

T. K. MENON: National Radio Astronomy Observatory, P.O. Box 2, Green Bank, WV 24944